Spectroscopic Probing of the Microenvironment in a Protein−Surfactant Assembly

Uttam Anand, Chandrima Jash, and Saptarshi Mukherjee*

Department of Chemical Sciences, Indian Institute of Science Education and Research Bhopal, ITI Campus (Gas Rahat) Building, Govindpura, Bhopal 462 023, Madhya Pradesh, India

Received: July 19, 2010; Revised Manuscript Received: October 15, 2010

The effect of the anionic surfactant sodium dodecyl sulfate (SDS) on the protein human serum albumin (HSA) was studied using steady-state spectroscopy, time-resolved measurements, and circular dichroism spectroscopy. The binding of SDS to the domain IIA of HSA, housing the single tryptophan amino acid residue (Trp214), was monitored, and it was found that this addition of the surfactant takes place in a sequential manner depending upon the concentration of the added surfactant. Both fluorescence intensity and lifetimes of HSA decreased with the increasing concentration of SDS, and the surfactant molecules serve the role of a quencher for the fluorescence of Trp214. Circular dichroism data also support the structural changes induced by SDS. The 17 disulfide bridges present in HSA provide the necessary structural rigidity to the protein. Stern−Volmer plots and thermodynamic parameters have been used to characterize the sequential binding of SDS to HSA, and these parameters not only confirm that the binding is spontaneous in nature but also is quite strong, depending on the concentration of the added surfactant.

Introduction

Human serum albumin (HSA) is the most abundant protein in the circulatory system and is responsible for the binding and transport of a wide variety of fatty acids, drug molecules, and metabolites to their molecular targets.[1] It is a single polypeptide chain having 585 amino acid residues, characterized by low tryptophan and high cysteine content.[2−4] The secondary structure of the protein consists of 67% α-helix, having 6 turns and 17 disulfide bridges from 35 cysteine moieties.[5] Under physiological conditions, HSA adopts a heart-shaped three-dimensional structure having three homologous domains I−III.[2,3] Each of these three domains are further subdivided into two subdomains A and B that consist of four and six α-helices, respectively.[1,2] Using X-ray crystallography, He and Carter showed that the two halves of the albumin molecule form a 10 Å wide and 12 Å deep crevice that houses a single tryptophan Trp214 residue in the binding site IIA of the protein.[2]

Interaction of proteins with surfactants, drug molecules, and denaturants is well documented and has been a topic of burgeoning interest.[6−12] At a high surfactant concentration, the three-dimensional structure of a protein is destroyed and the protein is said to be denatured. However, in 1948 Duggan and Luck[10] showed that the urea-induced denaturation of proteins may be prevented by the addition of a small amount of SDS. Moriyama and Takeda[6a] proposed that the secondary structure of HSA remains more or less unchanged with the addition of up to 0.2 mM of SDS. More recently, using circular dichroism spectroscopy, they have studied the effect of interaction of the double-tailed surfactant, sodium bis(2-ethylhexyl) sulfosuccinate (AOT) on the structure of HSA.[6b] They have shown that although the helicity of HSA decreased from 66% to 44% at 65 °C in the absence of AOT, low concentrations of AOT, however, prevent such decrement in the helicity of HSA thereby establishing the protective nature of the surfactant.[6b] The 17 disulfide bridges from 35 cysteine residues present in HSA[4] play a very significant role in accounting for the structural rigidity of the protein.[6c] Bhattacharyya and co-workers have studied the interaction of HSA with a very low concentration of SDS (80 μM) and have shown that when SDS binds to HSA, the solvation dynamics become faster, which is attributed to the displacement of the bound water molecules by SDS in the immediate vicinity of the fluorescent probe, TNS.[7a] In another work they have shown that the solvation dynamics of the probe CPM [7-(dimethylamino)-3-(4-maleimidophenyl)-4-methylcoumarin] covalently attached to HSA become faster by 1.3 times in the presence of SDS due to the binding of SDS to HSA.[7b] Using two model drugs, chlorin *p6* and purpurin 18, for photodynamic therapy, the specific binding in the vicinity of Sudlow's site I of HSA has been investigated.[11] Fluorescence resonance energy transfer (FRET) between the fluorescent dye, prodan, and tryptophan in guanidine hydrochloride-induced denatured HSA has been used to decipher the conformational changes.[12a] Panda and co-workers also studied the unfolding process of the three domains of HSA using covalently bound fluorescence probes and opined that the unfolding of these domains, induced by guanidine hydrochloride (GdnHCl), is sequential in nature.[12b] The uniqueness of HSA lies in the fact that it contains only one Trp214 located in its domain IIA that can be used as an intrinsic probe for studying the conformational changes in the protein molecule.[13−15] Trp214 is known to be located in the hydrophobic protein pocket consisting of the Lys(212)-Ala(213)-Trp(214)-Ala(215)-Val(216)-Ala(217)-Arg(218) chain of amino acids.

We have used steady-state, time-resolved measurements and circular dichroism spectroscopy in characterizing the mechanistic pathway of the interaction of the protein with the added surfactant molecules. Steady-state as well as the lifetime data clearly show that there are four stages of binding of the added SDS to the domain IIA of HSA molecules (depending upon the concentration of the surfactant), and this has been supported by the Stern−Volmer plots.[16] At very low concentrations of SDS (≤0.2 mM), the added surfactant molecules bind exclusively to the highly energetic sites of the protein molecules, and this binding is specific in nature.[17] As suggested by

* Corresponding author. E-mail: saptarshi@iiserbhopal.ac.in.

10.1021/jp106703h
Published on Web 11/15/2010

Moriyama and Takeda,[6a] the secondary structure of the protein remains almost unchanged up to this point. At such concentrations of SDS, the monomeric forms of the surfactant get preferentially attached on the peripheral sites of the globular protein.[18,19] Upon slowly increasing the concentration of SDS, the added surfactant molecules bind to the protein in a noncooperative manner characterized by a lower binding constant (K) and free energy of binding ($\Delta G^0_{binding}$).

Upon increasing the concentration of SDS in solution, the added surfactant molecules start aggregating and form micellar-like aggregates at around 7 mM SDS concentration. The protein polypeptide, linked by many disulfide bridges, cannot wrap around micelles of ionic surfactants, such as SDS. Such a polypeptide is absolutely different from single-chain polymers comprising simple repetition units. As aptly explained by Takeda and Moriyama,[20] the polypeptides of the intact BSA (note that HSA almost has a similar crystal structure) and many other proteins do not wrap around the SDS micelles. It is rather rational to conceive that such polypeptides most probably cannot form a helical structure around the micelle as suggested by other works on protein−surfactant assemblies.[8b,17]

Experimental Section

Materials. Human serum albumin (HSA) was purchased from Sigma, essentially fatty acid free and globulin free. Sodium dodecyl sulfate, SDS, was also purchased from Sigma and was used as received. All solutions were prepared in 50 mM Tris buffer, pH = 7.5. The temperature during all experiments was maintained at 25 °C ± 0.1 °C, unless otherwise mentioned.

Steady-State Measurements. Steady-state absorption measurements were carried out in a Perkin-Elmer UV−vis spectrophotometer, Lambda-25. All the steady-state fluorescence measurements were recorded on a Horiba Jobin Yvon, Fluorolog 3-111. A 50 μM (= 5 × 10^{-5} M) HSA solution was used to record the spectra in a 50 mM Tris buffer solution having a pH = 7.5. The concentration of the protein was determined spectrophotometrically using λ_{280} = 44 000.[6f] The final protein concentration was adjusted to 50 μM (= 5 × 10^{-5} M) for steady-state and lifetime measurements. The fluorescence spectra were measured with a 10 mm path length quartz cuvette. HSA was excited at 295 nm in order to minimize the contribution from tyrosine. The fluorescence emission was collected from 310 to 500 nm with an integration time of 0.1 s. The emission and the excitation slits were kept at 5 and 1.5 nm, respectively.

Time-Resolved Fluorescence Measurements. For lifetime measurements, the samples were excited at 295 nm using a picosecond diode (IBH-NanoLED source N-295). The emission was collected at magic angle polarization using a Hamamatsu MCP photomultiplier (Model R-3809U-50). The time-correlated single photon counting (TCSPC) set up consisted of an Ortec 9327 pico-timing amplifier. The data were collected with a PCI-6602 interface card as a multichannel analyzer. The typical full width at half maximum (fwhm) of the system response was about 810 ps.

Circular Dichroism Spectroscopy Measurements. Circular dichroism (CD) measurements were carried out on an Applied Photophysics (UK) (Model: CIRASCAN) spectropolarimeter equipped with a Peltier temperature controller. All the CD measurements were performed at 25 °C with an accuracy of ±0.1 °C. Spectra were collected with a scan speed of 200 nm/min with a spectral bandwidth of 10 nm. Each spectrum was the average of three scans. Secondary structure (far-UV CD) was measured over the wavelength range of 200−250 nm using a 0.1 cm path length cuvette. Buffer solutions containing the corresponding concentration of surfactants were subtracted from all the measurements. The results were expressed as mean residue ellipticity (MRE) in deg·cm^2 $dmol^{-1}$ which is defined as

$$\mathrm{MRE} = \frac{\theta_{obs} M}{nlC} \quad (1)$$

where θ_{obs} is the CD in millidegrees, M is the molecular weight of the protein in g $dmol^{-1}$, n is the number of amino acid residues (585 in the case of HSA), l is the path length (0.1 cm) of the cuvette, and C is the concentration of the protein in g L^{-1}.

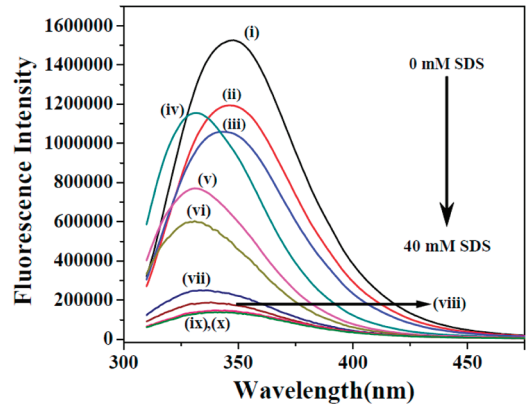

Figure 1. Fluorescence spectra of HSA in the absence and presence of SDS of various concentrations. (i) HSA in the absence of SDS. (ii−x) The emission spectra of HSA in the presence of 0.1 mM, 0.2 mM, 0.8 mM, 2 mM, 5 mM, 7 mM, 8 mM, 15 mM, and 40 mM SDS, respectively. The samples were excited at 295 nm to minimize the contribution of tyrosine.

Results and Discussion

Fluorescence Quenching of HSA in the Presence of SDS. The absorption spectra of the protein (HSA) alone and the protein−surfactant (HSA+SDS) assembly with varying concentrations of SDS were almost similar. The emission maximum of HSA alone in Tris buffer was found to be centered at 348 nm. Upon addition of SDS up to 0.2 mM, there is almost no shift in the emission maximum, whereas the fluorescence intensity decreases by 30% (Figure 1). In terms of the area under the curve, similar results were obtained where the area decreases by about 31% up to 0.2 mM SDS. This is a clear signature of the fact that the secondary structure of the protein HSA remains almost unaltered up to 0.2 mM SDS as reported earlier by Moriyama and Takeda.[6a] Because there is no shift in the emission maximum, it can be concluded that the fluorophore Trp214 experiences more or less the same environment up to 0.2 mM SDS. At very low concentrations of SDS, the added surfactant molecules bind exclusively to the highly energetic sites of the protein, and this binding is specific in nature. The secondary structure of the protein remains almost intact, and its tertiary structure starts opening up.

Fluorescence quenching has been widely used as a powerful tool to unravel the mechanistic pathway of the accessibility of the protein molecule to the quencher(s) present. The quenching of fluorescence is known to occur by two processes, namely collisional (dynamic) quenching and/or formation of a complex between the quencher and fluorophore (static quenching).[16] The fluorescence quenching data were analyzed according to the Stern−Volmer equation:[11,16]

$$F_0/F = 1 + K_{SV}[Q] \quad (2)$$

In the above equation, F_0 and F are the fluorescence peak intensities of the fluorophore (Trp214 in HSA) in the absence and presence of quencher. [Q] is the quencher (SDS in the present case) concentration, and K_{SV} is the Stern−Volmer quenching constant. Besides estimating the magnitude of quenching using eq 2, we can further estimate the binding constant (K) and the binding affinity (n). For this purpose we use a modified version of the Stern−Volmer equation as given by:

$$\log[(F_0 - F)/F] = \log K + n \log[Q] \quad (3)$$

The thermodynamics of binding can be estimated by measuring the free energy of binding ($\Delta G^0_{binding}$) given by:

$$\Delta G^0_{binding} = -2.303RT \log K \quad (4)$$

A plot of $\log[(F_0 - F)/F]$ against log[SDS] is shown in Figure 2. From the figure it is evident that the binding of SDS to HSA takes place in distinct stages as marked by regions I−IV in Figure 2. Using eqs 3 and 4, the magnitudes of K, n, and $\Delta G^0_{binding}$ have been estimated for the first three regions (I−III of Figure 2 up to which binding of SDS to HSA takes place) and are summarized in Table 1. The inset of Figure 2 shows a representative plot of log $[(F_0 - F)/F]$ against log[SDS] corresponding to region III of Figure 2. The stepwise addition and sequential unfolding of HSA, induced by GdnHCl, has been studied by Panda and co-workers[12b] where they suggest that domain II undergoes unfolding prior to domain I which is followed by domain III of HSA. Figure 3a shows the Stern−Volmer plot up to 0.2 mM SDS corresponding to region I of Figure 2. The values of all the thermodynamic parameters and quenching constant (as seen in Table 1) indicate that the binding during this region is not only spontaneous but also very strong as indicated by the magnitude of K and $\Delta G^0_{binding}$. From the magnitude of n we can conclude that the affinity of SDS toward HSA is rather strong in this concentration range.

Upon slowly increasing the concentration of SDS beyond 0.2 mM, the hydrophobicity in and around the Trp214 region increases. This is manifested by the 16 nm blue shift in the emission maxima which shifts from 348 to 332 nm at 7 mM SDS concentration (Figure 1), and the fluorescence intensity also decreases further by 75%. The area under the emission graphs shows a similar decrement on increasing the SDS concentration from 0.2 to 7 mM. The blue shift in emission maxima clearly suggests that the Trp214 inside the HSA is experiencing a more hydrophobic environment due to the presence of the alkyl chains of the surfactant molecules. This stage of binding of SDS to HSA is noncooperative in nature and is shown by the plateau region II of Figure 2. The values of K, n, and $\Delta G^0_{binding}$ for region II are very small as compared to that of regions I and III (Table 1). Using a protein concentration of 10 μM, Takeda and co-workers have studied the binding of SDS to the protein and they have proposed that micelle-like aggregates start forming beyond 1 mM SDS concentration.[6c,f] In our present work we have used a protein concentration of 50 μM, and we observed that the SDS surfactant molecules start forming such micelle-like aggregates at around 7 mM SDS concentration, in agreement to what has been observed by Takeda and co-workers. This local aggregation

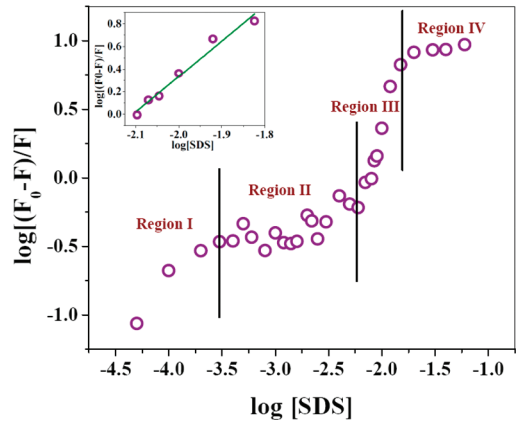

Figure 2. A plot of log $[(F_0 - F)/F]$ against log[SDS] as per the modified Stern−Volmer equation. F_0 and F are the peak fluorescence intensities of HSA in the absence and presence of quencher, SDS. The regions (I−IV) represent the various binding stages of SDS to HSA. The inset shows a representative plot corresponding to region III.

TABLE 1: Quenching Constants and Thermodynamic Parameters of HSA+SDS Assembly

region	K_{SV} (L mol^{-1})	K (M^{-1})	n	$\Delta G^0_{binding}$ (kJ mol^{-1})
region I	2.33×10^3	1.51×10^4	1.21	−23.84
region II	73.84	2.36	0.26	−2.12
region III	8.53×10^2	3.97×10^6	3.13	−37.65

of the surfactant molecules is well exemplified from the breakpoint of the end of region II of Figure 2. Note that upon SDS binding, the protein−surfactant assembly swells in size[6c] and as a consequence there is an increase in the number of available binding sites.[18]

The binding in region III (Figure 2) is highly cooperative in nature and the added surfactant molecules attaches to the protein in a cooperative manner. The binding of SDS molecules to HSA results in the availability of more binding sites as the region in and around Trp214 becomes a bit more exposed and hence the term "cooperative binding" is coined. As explained by Panda and co-workers,[12b] when HSA unfolds, it is domain II that initiates the process. As Trp214 is housed in domain IIA, the added surfactant molecules bind exclusively in and around the Trp214 which is facilitated by the unfolding of domain II. The emission maximum now shows a red shift of about 12 nm (shifting from 332 to 344 nm). The emission intensity also further decreases by 44%, and the area under the curve also shows a similar trend. The red shift in the emission maxima is a manifestation of the more hydrophilic environment as experienced by the Trp214 residue, as the protein undergoes some sort of distortion thereby making the microenvironment near the Trp214 more polar. The magnitudes of K_{SV}, K, n, and $\Delta G^0_{binding}$ for region III are summarized in Table 1. Figure 3b shows the Stern−Volmer plot up to 15 mM SDS corresponding to region III of Figure 2. It is evident that the starting point of the curve corresponds to the end of region II of Figure 2 which serves as the initial point for Figure 3b. During this concentration range, the process of binding is very strong (characterized by the highest K value) and it supersedes the process of quenching as manifested from the values of K_{SV} and K unlike what is seen in region I. The high magnitude of the free energy of binding supports that this binding is very spontaneous in nature. Also, the magnitude of n suggests that the binding affinity of SDS toward HSA is the strongest in region III. Trp214 is known to be located in the hydrophobic protein pocket consisting of the Lys(212)-Ala(213)-Trp(214)-Ala(215)-Val(216)-Ala(217)-Arg(218) chain of amino acids. When SDS is added in low

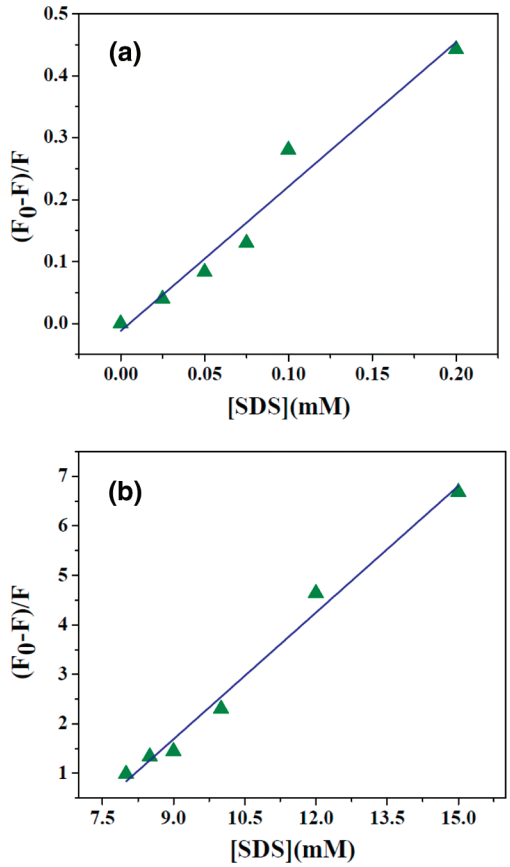

Figure 3. (a) Stern−Volmer plot of region I in Figure 2 representing a concentration range of 0−0.2 mM SDS. (b) Stern−Volmer plot of region III in Figure 2 representing a concentration range of 8−15 mM SDS.

concentrations, the interactions of Lys(212) and Arg(218) amino acid residues with the dodecyl sulfate anion causes a strong change in the nearest environment of Trp214. This specific and noncooperative interaction on one hand exhibits a blue shift and on the other hand causes a partial opening of the hydrophobic pocket with Trp214. During this region, the secondary structure of HSA predominantly changes, and this is in excellent agreement to the observations of Takeda and co-workers.[6c]

Finally, at very high SDS concentrations (region IV of Figure 2), the process is mostly noninteractive in nature and the addition of SDS to HSA gets almost saturated. The added surfactant molecules show almost no affinity of binding toward HSA. The emission maximum and the fluorescence intensity more or less remain unchanged during region IV. Because the fluorescence intensity does not decrease much (∼1%), we may propose that the quenching is dynamic in nature which is characterized by a low K_{SV} value of 27.04 L mol^{-1}. As mentioned earlier, that the binding of SDS to HSA almost ends beyond 15 mM SDS; hence, we did not estimate the magnitudes of the binding constant (K) and free energy of binding ($\Delta G^0_{binding}$).

Time-Resolved Fluorescence Quenching of HSA in the Presence of SDS. The investigation of intrinsic fluorescence from proteins has been regarded as an effective method to study protein conformational dynamics. Protein fluorescence can be complex as well as very challenging to explain, but has been a topic of interest of late. Despite the fact that the structure of HSA is rather complicated, it has been widely studied by making use of the single Trp214 residue which is used as an intrinsic fluorophore. In aqueous solutions at neutral pH, Trp214 exhibits multiple exponential decays, and this has been attributed to the existence of rotational conformational isomers, called rotamers.[16] Fleming and co-workers[21] have studied the fluorescence decays of Trp214 in terms of a simple model based on the conformers about the $C^{\alpha}-C^{\beta}$ bond and the relative rates of charge transfer from indole to the various electrophiles. It is believed that three conformers of Trp214 can be present as shown below:[16,21]

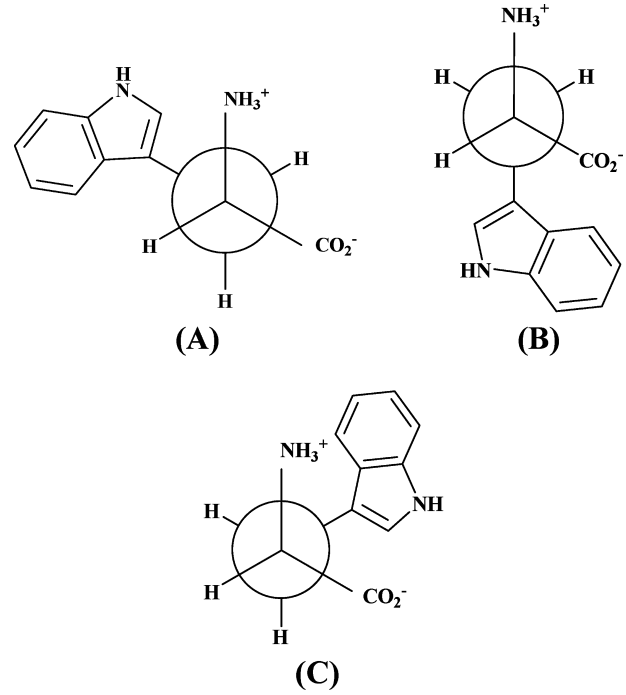

It is thought that conformer C is rather stable and conversion from C to either A or B is difficult on a nanosecond time scale.[22] Because Trp214 exhibits multiexponential decays in aqueous solutions, the faster component can be attributed to the existence of the conformer C, whereas the longer lifetime mainly arises from the rapidly interconverting A and B conformers. The contribution of these lifetimes has been ascribed to the relative populations of the various conformers present in the system.[23] Although solvation plays a major role in determining the Trp214 fluorescence, however, chemical moieties such as ionic species, disulfide bonds, methionyl sulfur, etc., also play a significant role in controlling the emission properties because of their quenching abilities. It is also believed that the indole ring is slightly puckered in the ground state but becomes planar in the excited state which presumably reflects delocalization during the excited state of the lone pair of electrons on the nitrogen into the aromatic system.[23] During the process of quenching, interactions of the quencher molecules with the substrate lead to the distortion of the indole ring planarity thereby changing the local environment around the Trp214 and causing a decrement in the lifetime.

In our present work, we studied the effect of addition of SDS to a 50 μM HSA solution in buffer by measuring the lifetimes of Trp214 under various concentrations of SDS. For lifetime measurements, the samples were excited at 295 nm using a picosecond diode laser, and the fluorescence decays of HSA and HSA+SDS assembly were monitored at the respective emission maximum of the systems. Figure 4 shows representative decays of HSA in buffer, HSA in the presence of 1.2 mM, and 40 mM SDS. It can be easily seen that the lifetime of Trp214 in HSA is gradually decreasing upon the addition of SDS, as

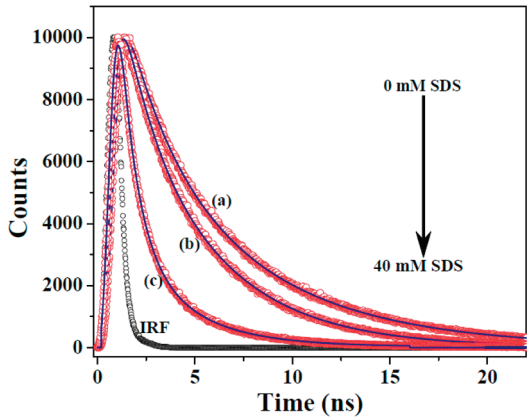

Figure 4. Fluorescence lifetime decays of HSA (a) in the absence of SDS, (b) in the presence of 1.2 mM SDS, and (c) in the presence of 40 mM SDS. The scattered points represent the actual decay profile while the solid blue line represents a biexponential fit to that decay.

TABLE 2: Fluorescence Lifetimes of HSA as a Function of Concentrations of SDS

SDS (mM)	a_1	τ_1 (ns)	a_2	τ_2 (ns)	$\langle\tau\rangle^a$ (ns)	$\chi^{2\,b}$
0	0.18	2.40	0.82	6.51	5.78	1.08
0.2	0.21	2.19	0.79	5.97	5.19	1.17
0.4	0.15	1.81	0.85	4.71	4.28	1.05
2.5	0.15	1.96	0.85	4.64	4.24	1.10
4.0	0.17	1.23	0.83	4.57	4.15	1.20
7.0	0.37	1.23	0.63	3.98	2.97	1.15
8.0	0.38	0.01	0.62	3.48	2.15	1.22
10.0	0.41	0.009	0.59	3.14	1.86	1.23
40.0	0.42	0.009	0.58	3.03	1.75	1.25

[a] $\langle\tau\rangle = a_1\tau_1 + a_2\tau_2$. [b] The magnitude of χ^2 denotes the goodness of the fit.

the latter is responsible for quenching the fluorescence. Table 2 summarizes the decay parameters of the protein and protein−surfactant assembly at some of the concentrations of SDS. From the lifetime values, the stepwise addition of SDS to HSA is also well exemplified. It is very interesting to note that the lifetime values also support the stepwise mechanism of the addition of SDS leading to the formation of the protein−surfactant assembly as shown in Figure 2. The average lifetime of HSA reduces from 5.78 to 1.75 ns in the absence and presence of 40 mM SDS. The reduction of lifetime is a manifestation of both quenching triggered by SDS as well as due to conformational transitions in Trp214. The average lifetime of HSA in the presence of 0.2 mM SDS shows marginal reduction, and we may attribute this small decrement to the change in the tertiary structure of the protein keeping the secondary structure almost intact, as discussed earlier. During the concentration range corresponding to region I, the process of quenching brought about by the SDS molecules is the driving force and, consequently, the binding process is less predominant as compared to region III. Beyond 0.2 mM SDS, the process of noncooperative binding leading to the partial opening of the secondary structure continues which is followed by cooperative binding as corroborated in regions II and III of Figure 2. The dynamic process of quenching further reduces the average lifetime from 5.2 ns (for 0.2 mM SDS) to around 3 ns (for 7 mM SDS). During this region, the added surfactant molecules bind to the protein near the Trp214 and start forming local aggregates of micelle-like structures at 7 mM SDS. Beyond 7 mM SDS, the protein−surfactant assembly swells and the Trp214 experiences a more hydrophilic (polar) environment. Here the added surfactant molecules show cooperative binding

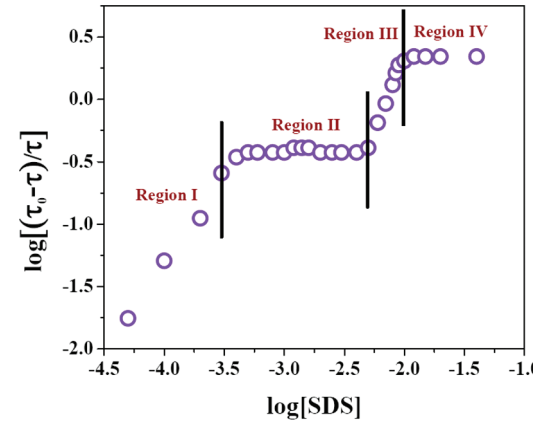

Figure 5. A plot of $\log[(\langle\tau\rangle_0 - \langle\tau\rangle)/\langle\tau\rangle]$ against log[SDS] as per the modified Stern−Volmer equation. $\langle\tau\rangle_0$ and $\langle\tau\rangle$ are the average lifetime values of HSA in the absence and presence of quencher, SDS. The regions (I−IV) represent the various binding stages of SDS to HSA.

between the concentration range of 7 mM to 15 mM SDS. As explained in the above section, the secondary structure of the protein predominantly changes, thereby possibly exposing the hydrophobic cavity and leading to a decrement of lifetime from 3 to 1.78 ns in the presence of 7 mM and 15 mM SDS, respectively (Table 2). The binding becomes almost saturated beyond 15 mM SDS, and most probably the quenching of fluorescence intensity is dynamic in nature, as the lifetime value shows a marginal decrease from 1.78 ns (in the presence of 15 mM SDS) to 1.75 ns (in the presence of 40 mM SDS).

In order to support the mechanistic pathway of the addition of SDS to HSA, we have used the average lifetime values instead of fluorescence intensities in analogy with eq 3 as:

$$\log[(\langle\tau\rangle_0 - \langle\tau\rangle)/\langle\tau\rangle] = \log K + n \log[\mathrm{Q}] \qquad (5)$$

where $\langle\tau\rangle_0$ and $\langle\tau\rangle$ represent the average lifetime values of HSA in the absence and presence of SDS. A plot of $\log[(\langle\tau\rangle_0 - \langle\tau\rangle)/\langle\tau\rangle]$ against log[SDS] is shown in Figure 5. Interestingly, we again observed four distinct regions (as marked in the figure) exemplifying that the binding of SDS is sequential in nature, in similar lines to what we observed from steady-state fluorescence data.

Although it is very difficult to ascribe the individual contributions of lifetime in a multiexponential decay as observed in the present case of protein−surfactant assembly, we will make an effort to explain the relative amplitudes of the lifetimes. The contribution of these lifetimes has been mainly ascribed to the relative populations of the various conformers present in the excited state. From the magnitudes of the relative contributions of lifetimes, it may be suggested that the contribution from conformer C is around (18 ± 3) % whereas that from conformers A and/or B is around (82 ± 3) %. As mentioned earlier, the shorter lifetime has been attributed to conformer C whereas the longer lifetime was thought to be from the rapid interconverting A and B conformers.[22] Once micelle-like aggregates are formed, the contributions of the relative amplitudes suddenly change and the contribution from conformer C rises to around (40 ± 3) % whereas that from conformers A and/or B decreases to about (60 ± 3) %. In the absence of any quencher, HSA contains 67% of α-helix and at low concentrations of SDS the secondary structure remains almost intact and rigid. Hence, the planarity and rotation of indole is hindered, making the lifetime values high. At SDS concentrations less than 7 mM, the interconversion

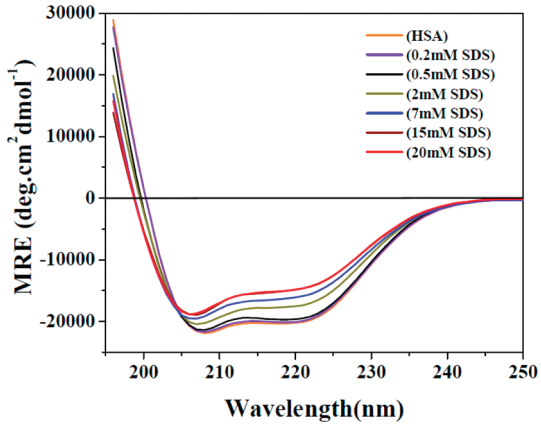

Figure 6. Circular dichroism (CD) spectra of HSA in the absence of SDS and in the presence of increasing concentrations of SDS. The concentrations of the SDS used are marked in the figure.

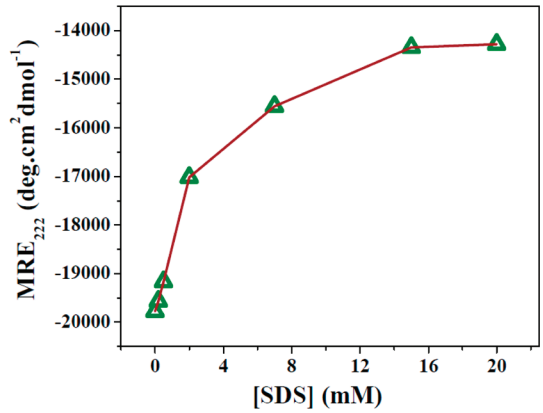

Figure 7. Plot of mean residue ellipticity (MRE) of HSA at 222 nm against [SDS].

from conformer C to A or B is not that easy, as the protein still contains most of its secondary structure intact. Trp214 still experiences a constrained environment, and the region in and around it remains relatively nonpolar; hence, the lifetime is seen to be high. Beyond the concentration where the SDS molecules form local micelle-like aggregates, the protein−surfactant assembly swells and hence the Trp214 experiences a more polar and nonconstrained environment. As a consequence of this loss in rigidness, the conversion from conformers A and/or B is enhanced, reducing the relative amplitude of the longer lifetime. The ring planarity also increases and rotation of the indole is facilitated, making the contribution from the conformer C more prominent as seen by the increment in the relative amplitude of the shorter lifetimes. The nonradiative pathways in Trp214, mainly the charge transfer process from the indole ring to a nearby substituent, are enhanced and thus shorten the lifetime.

Circular Dichroism Spectra. Circular dichroism (CD) spectroscopy is widely used to monitor the structure, conformation, and stability of proteins in solutions.[6a,b,d,f,12b,23−27] CD probes the secondary structure of proteins because the peptide bond is asymmetric and molecules without a plane of symmetry show the phenomena of CD. Although CD cannot provide the details regarding the precise structure of proteins (as it is supposed that fluorescence techniques are rather more sensitive in deciphering small changes in molecular level), nevertheless, it can provide us with a very good estimation of the fraction of the residues in the protein structure which are involved in α-helix, β-sheet, and disorderly formation (random coil). In order to decipher the structural and conformational changes brought in by the added SDS molecules, we have performed CD spectral studies of HSA in the presence of varying concentrations of the surfactant, SDS. Figure 6 shows the CD spectra of HSA both in the absence and presence of SDS of varying concentrations. It is evident from the figure that the CD spectra show two minima at 208 and 222 nm, which is a clear signature of the presence of α-helix in the protein under study. It has been reported that HSA contains around 65−67% α-helix in its native form.[6a,b,18,25] Although high concentrations (40 mM) of SDS bring about structural deformation of HSA, it has been proposed that the helical structure remains almost 90% intact.[25] This clearly suggests that even in the presence of high concentrations of SDS, the 17 disulfide bonds are not broken or reduced, as correctly proposed by Takeda and Moriyama.[20] It is important to remember that the CD results only give us an estimate of the global structural changes induced by the surfactant and surely do not provide us with the details of the microenvironmental changes induced.

For CD measurements, the HSA concentration was kept at 5 μM (= 5 × 10^{-6} M, determined spectrophotometrically as explained in the Experimental Section) and a cell of 0.1 cm path length was used to record the spectra. However, the SDS concentrations were kept same as those used in other steady-state and time-resolved experiments. We have analyzed our CD data and obtained an α-helical content of about 67% in HSA in the absence of SDS (using software downloaded free from the Internet (www.embl.de/~andrade/k2d/)). This value agrees very well with that of the reported literature.[5,6a,b,18,25] In order to investigate the effect of the added SDS on the structure of HSA, we have plotted a graph of MRE_{222} (ellipticity at 222 nm) against the [SDS] as shown in Figure 7. From the figure it is evident that the helicity of HSA almost remains constant up to 0.2 mM SDS and shows marginal decrease (~3%) at 0.5 mM SDS, confirming that the structural changes have already been induced at this SDS concentration. The CD spectroscopy probes the changes in the secondary structure of the entire HSA molecule brought in by the added SDS molecules. Using a protein concentration of 50 μM (in steady-state and time-resolved experiments), we observed that micelle-like assemblies start forming at around 7 mM SDS. However, similar aggregates are formed at much lower concentrations when carrying the CD experiments using 5 μM HSA. From Figure 7 it is evident that the secondary structure of HSA continues to change until about 15 mM SDS, beyond which there are no observable changes. At 15 mM SDS, the ellipticity of HSA at 222 nm changes by about 27% as seen from Figure 7. This can be attributed to the fact that when SDS is added to HSA, CD probes the structural changes of the entire protein as a whole. Unlike in steady-state and time-resolved studies, we probe the interaction of SDS with Trp214 of HSA, and hence the SDS serves as a quencher when it binds to Trp214. Comparing Figures 2 and 5 with Figure 7, we can conclude that the addition of SDS is sequential in nature; however, there is no direct correspondence between the steady-state and time-resolved data (as obtained from Figures 2 and 5) with that obtained from CD spectra (as obtained from Figure 7). This is mainly because in steady-state and time-resolved studies, we are using an HSA concentration that is 10 times higher than that used in CD studies. Also, as mentioned earlier, SDS serves to quench the fluorescence of Trp214 as it attaches to domain IIA, whereas in CD spectra we monitor the overall structural changes of the protein induced by SDS.

Conclusion

The binding of the surfactant SDS to the protein HSA has been studied very thoroughly, and the microenvironment of the

region in and around the Trp214 in HSA has been investigated. The SDS serves the role of a quencher and attaches to domain IIA housing Trp214. We conclude that this binding takes place in a sequential manner depending on the concentration of the surfactant used. Steady-state fluorescence data suggest that the quenching brought about by the added SDS makes the Trp214 experience various environments which are manifested by the emission maximum. Also, the decrement of lifetimes is an indication of the various conformational changes that the Trp214 undergoes. The seminal role played by the 17 disulfide bonds in providing the necessary structural rigidity to the protein has also been established.

Acknowledgment. We sincerely thank Professor Vinod Kumar Singh, Director IISER Bhopal for his constant encouragement and support. We also thank the Advanced Instrumentation Research Facility, Jawaharlal Nehru University (JNU), New Delhi, for helping us to carry out the CD spectroscopy experiment. S.M. thanks Dr. Sobhan Sen, School of Physical Sciences, JNU, New Delhi, for many stimulating discussions. U.A. and C.J. thank IISER Bhopal for providing fellowships.

References and Notes

(1) Peters, T. *All About Albumin: Biochemistry, Genetics, and Medical Applications*; Academic: San Diego, 1996.

(2) He, X. M.; Carter, D. C. *Nature* **1992**, *358*, 209.

(3) Brown, J. R.; *Albumin Structure, Functions and Uses*; Rosenoer, V. M.; Oratz, M.; Rothschild, M. A., Eds.; Pergamon Press: Oxford, U. K., 1977.

(4) Sugio, S.; Kashima, A.; Mochizuki, S.; Noda, M.; Kobayashi, K. *Protein Eng.* **1999**, *12*, 439.

(5) Narazaki, R.; Maruyama, T.; Otagiri, M. *Biochim. Biophys. Acta* **1997**, *1338*, 275.

(6) (a) Moriyama, Y.; Takeda, K. *Langmuir* **1999**, *15*, 2003. (b) Moriyama, Y.; Takeda, K. *Langmuir* **2005**, *21*, 5524. (c) Takeda, K.; Yamamoto, K. *J. Protein Chem.* **1990**, *9*, 17. (d) Moriyama, Y.; Ohta, D.; Hachiya, K.; Mitsui, Y.; Takeda, K. *J. Protein Chem.* **1996**, *15*, 265. (e) Wada, A.; Takeda, K. *J. Colloid Interface Sci.* **1990**, *138*, 277. (f) Moriyama, Y.; Kanasaka, Y.; Takeda, K. *J. Colloid Interface Sci.* **2003**, *257*, 41. (g) Moriyama, Y.; Watanabe, E.; Kobayashi, K.; Harano, H.; Inui, E.; Takeda, K. *J. Phys. Chem. B* **2008**, *112*, 16585.

(7) (a) Mukherjee, S.; Sen, P.; Halder, A.; Sen, S.; Dutta, P.; Bhattacharyya, K. *Chem. Phys. Lett.* **2003**, *379*, 471. (b) Mandal, U.; Ghosh, S.; Mitra, G.; Adhikary, A.; Dey, S.; Bhattacharyya, K. *Chem. Asian J* **2008**, *3*, 1430. (c) Sen, P.; Dutta, P.; Halder, A.; Mukherjee, S.; Sen, S.; Bhattacharyya, K. *Chem. Phys. Lett.* **2003**, *377*, 229. (d) Sahu, K.; Mondal, S. K.; Roy, D.; Karmakar, R.; Bhattacharyya, K. *Chem. Phys. Lett.* **2005**, *413*, 484. (e) Sahu, K.; Roy, D.; Mondal, S. K.; Karmakar, R.; Bhattacharyya, K. *Chem. Phys. Lett.* **2005**, *404*, 341.

(8) (a) Hazra, P.; Chakrabarty, D.; Chakraborty, A.; Sarkar, N. *Biochem. Bhiophys. Res. Commun.* **2004**, *314*, 539. (b) Chakraborty, A.; Seth, D.; Setua, P.; Sarkar, N. *J. Phys. Chem. B* **2006**, *110*, 16607.

(9) Mir, M. A.; Gull, M.; Khan, J. M.; Khan, R. H.; Dar, A. A.; Rather, G. M. *J. Phys. Chem. B* **2010**, *114*, 3197.

(10) Duggan, E. L.; Luck, F. M. *J. Biol. Chem.* **1948**, *172*, 205.

(11) Patel, S.; Datta, A. *J. Phys. Chem. B* **2007**, *111*, 10557.

(12) (a) Krishnakumar, S. S.; Panda, D. *Biochemistry* **2002**, *41*, 7443. (b) Santra, M. K.; Banerjee, A.; Rahaman, O.; Panda, D. *Int. J. Biol. Macromol.* **2005**, *37*, 200.

(13) Diaz, X.; Abuin, E.; Lissi, E. J. *Photochem. Photobiol., A* **2003**, *155*, 157.

(14) Santra, M. K.; Banerjee, A.; Krishnakumar, S. S.; Rahaman, O.; Panda, D. *Eur. J. Biochem.* **2004**, *271*, 1789.

(15) Brahma, A.; Mandal, C.; Bhattacharyya, D. *Biochim. Biophys. Acta* **2005**, *175*, 1159.

(16) Lakowicz, J. R. *Principles of Fluorescence Spectroscopy*, 3rd ed.; Springer: New York, 2006.

(17) Turro, N. J.; Lei, X.-G.; Ananthapadmanabhan, K. P.; Aronson, M. *Langmuir* **1995**, *11*, 2525.

(18) Chakraborty, T.; Chakraborty, I.; Moulik, S. P.; Ghosh, S. *Langmuir* **2009**, *25*, 3062.

(19) Takeda, K.; Moriyama, Y.; Hachiya, K. Interaction of Proteins with Ionic Surfactants. In *Encyclopedia of Surface and Colloid Science*; Marcel Dekker, Inc.: New York, 2002.

(20) Takeda, K.; Moriyama, Y. *J. Phys. Chem. B* **2007**, *111*, 1244.

(21) Pertich, J. W.; Chang, M. C.; McDonald, D. B.; Fleming, G. R. *J. Am. Chem. Soc.* **1983**, *105*, 3824.

(22) Szabo, A. G.; Rayner, D. M. *J. Am. Chem. Soc.* **1980**, *102*, 554.

(23) Alcala, J. R.; Gratton, E.; Prendergast, F. G. *Biophys. J.* **1987**, *51*, 597.

(24) Corrêa, D. H. A.; Ramos, C. H. I. *African J. Biochem. Res.* **2009**, *3*, 164.

(25) Parker, W.; Song, P.-S. *Biophys. J.* **1992**, *61*, 1435.

(26) Johnson, W. C., Jr. *Annu. Rev. Biophys. Biol.* **1988**, *17*, 145.

(27) Woody, R. W. Theory of Circular Dichroism of Proteins. In *Circular Dichroism and Conformational Analysis of Biomolecules*; Fasman, G. D., Ed.; Plenum Publishing Corp.: New York, 1996; p 25.

JP106703H